

Rain Contribution to Oceanic and Terrestrial Water Balance

W. Timothy Liu and Xiaosu Xie

Jet Propulsion Laboratory, California Institute of Technology, Pasadena, CA

Email: w.timothy.liu@jpl.nasa.gov



1. Atmospheric water balance

The equation of water balance in the atmospheric column is

$$\frac{\partial W}{\partial t} + \nabla \cdot \Theta = E - P = F \quad (1)$$

where

$$\Theta = \int_0^{p_s} q u dp \quad (2)$$

is the moisture transport integrated over the depth of the atmosphere, and

$$W = \frac{1}{g} \int_0^{p_s} q dp \quad (3)$$

is the precipitable water or column integrated water vapor. In these equations, p is the pressure, p_s is the pressure at the surface, q and u are the specific humidity and wind vector at a certain level. Bold symbols represent vector quantities. For period longer than a few days (residence time of water in atmosphere), $P = E - \nabla \cdot \Theta$.

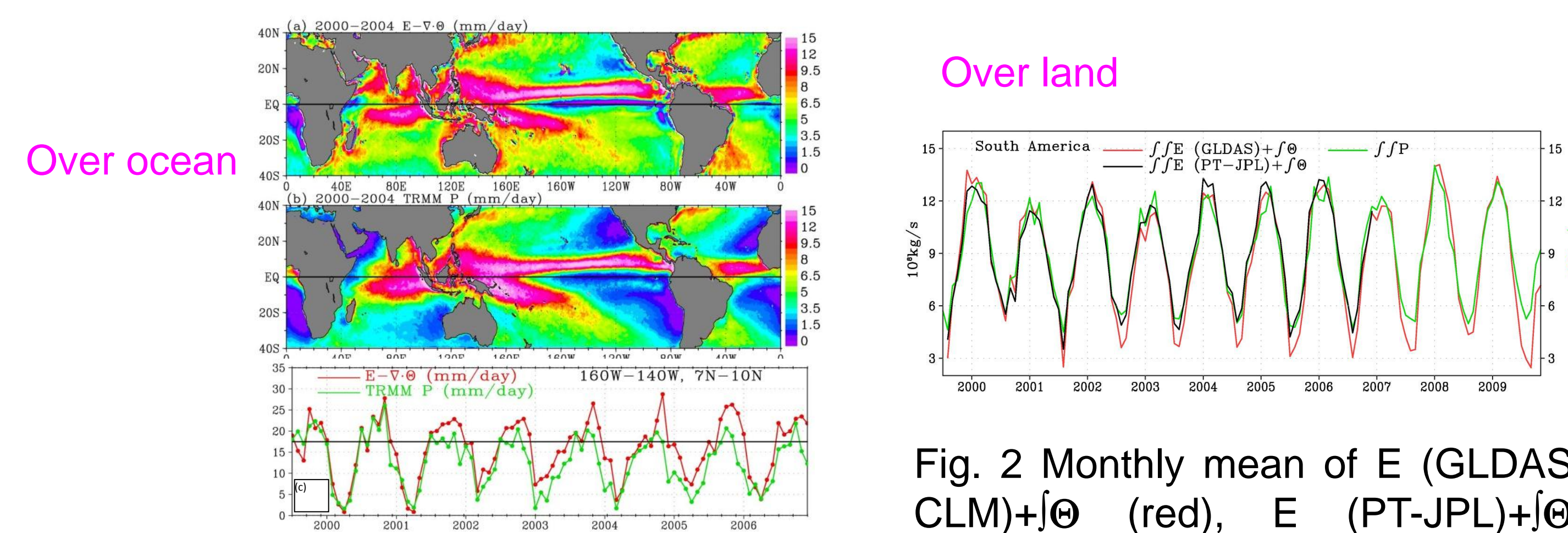


Fig. 1 Annual mean of (a) $E - \nabla \cdot \Theta$ and (b) P in mm/day, averaged from 2000-2004, derived from QuikSCAT, SSM/I, and TMI. (c) Monthly mean time series of $E - \nabla \cdot \Theta$ and P averaged between 160W-140W and 7N-10N.

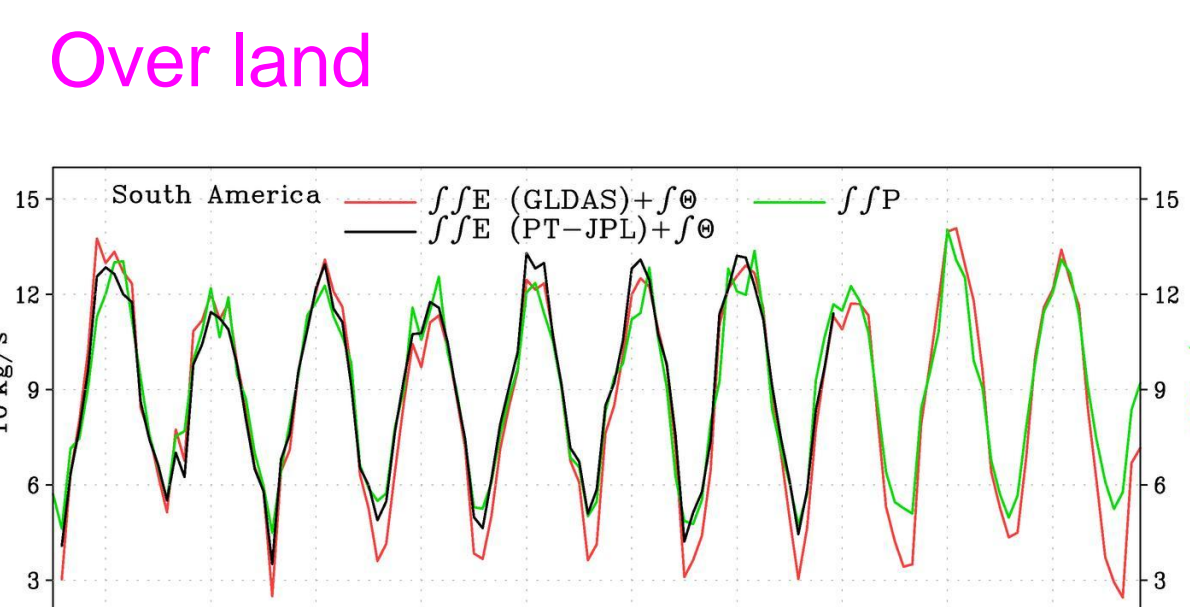


Fig. 2 Monthly mean of E (GLDAS CLM) + $\nabla \cdot \Theta$ (red), E (PT-JPL) + $\nabla \cdot \Theta$ (black), compared with P (green) from TRMM 3B42, integrated over South America. Two sets of E are used, one from model output, GLDAS (red), and the other derived from satellite data, PT-JPL (black).

TRMM data demonstrate near closure of atmospheric water balance over tropical ocean and land. GPM will provide global coverage and improvement over land. E over land is being improved with soil moisture measured by new L-band sensors.

2. Mass balance

Over global oceans, the sum of all river discharge from land (R) is balanced by the time change of mass ($\partial M / \partial t$) and surface water flux (F), integrated over all ocean area.

$$\int R = \int \left(\frac{\partial M}{\partial t} + F \right) \quad (4)$$

where \int and \iint represent line and area integrals, respectively. Similarly, over a continent or a river basin

$$\int R = - \left(\iint \left(\frac{\partial M}{\partial t} + F \right) \right) \quad (5)$$

where M is the mass of the continent or the river drainage basin and E is the evapotranspiration over land.

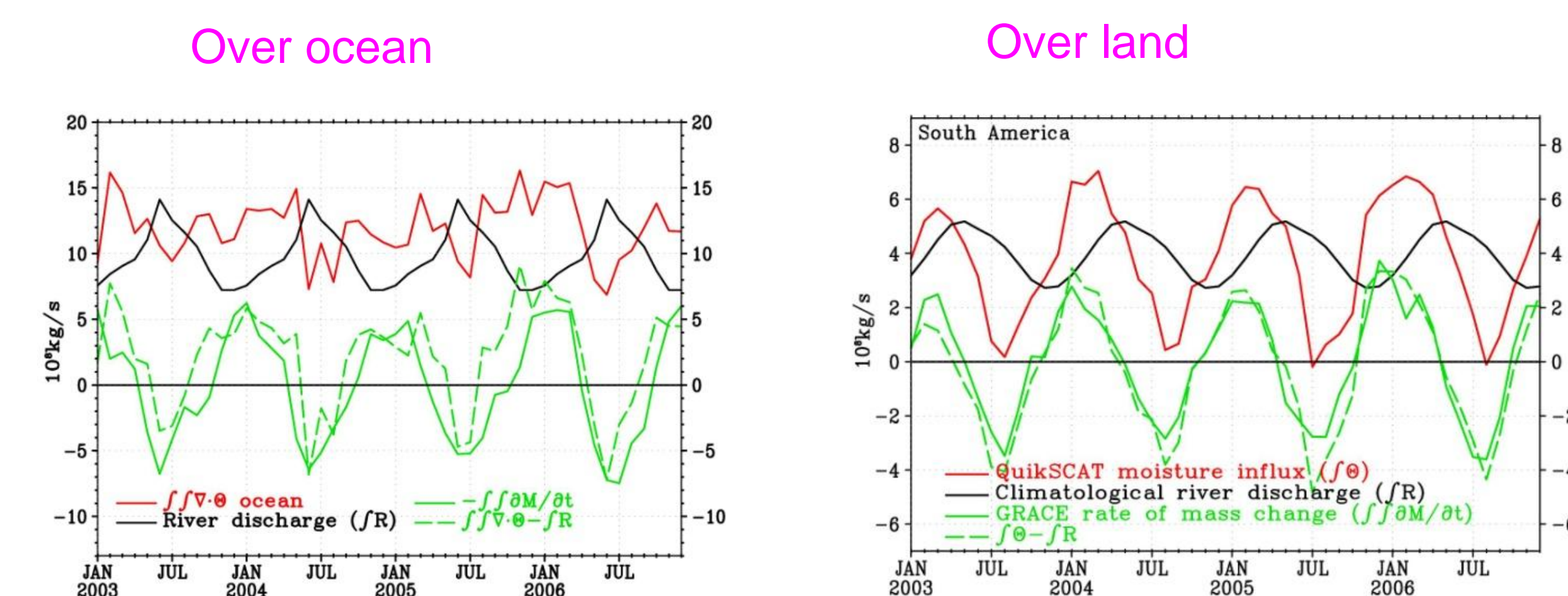


Fig. 3 Monthly mean of mass change rate $\int \partial M / \partial t$ (solid green line) from GRACE, freshwater flux $\int \nabla \cdot \Theta$ (red line), sum of climatological total river discharge across all coastline $\int R$ (solid black line), and $\int \nabla \cdot \Theta - \int R$ (dashed green line) over the global ocean.

Fig. 4 Monthly mean of mass change rate $\int \partial M / \partial t$ (solid green line), climatological river discharge $\int R$ (solid black line), total moisture transport across coastline into the continent $\int \Theta$ (red line), and $\int \Theta - \int R$ (dashed green line) over South America.

Fig. 3 shows that, over global ocean, the difference between F and R agrees with $\partial M / \partial t$ both in magnitude and in phase of annual variation, for the four-year period. The difference between $-\partial M / \partial t$ and $\nabla \cdot \Theta - \int R$ has a mean of 2.1×10^8 kg/s and a standard deviation of 2.6×10^8 kg/s. The standard deviation is 18% of the peak-to-peak variation of 12×10^8 kg/s. Over the continent of South American (Fig. 4), $\int \Theta - \int R$ agrees, both in phase and in magnitude, with $\int \partial M / \partial t$. The standard deviation of the difference is 0.9×10^8 kg/s, which is 7% of the peak-to-peak variation of 13×10^8 kg/s.

3. Amplification of water cycle, expansion of Hadley cell, and change in atmospheric river under global warming

Three hypotheses:

- (1) Wet region gets wetter and dry region gets drier
- (2) Hadley cell expansion
The poleward boundaries of the Hadley cell are defined as the boundary between easterly and westerly winds and between positive and negative $E - P$.
- (3) Atmospheric river intensifies
We describe atmospheric river using Θ .

Fig. 5 Time series of $\nabla \cdot \Theta$ averaged over (a) 150°W-140°W, 15°N-25°N, (b) 100°W-90°W, 22°S-10°S, and (c) 150°W-140°W, 7°N. Linear slope (green line) and standard error of the slope are marked at the top, with green color above and blue color below the 95% confidence level.

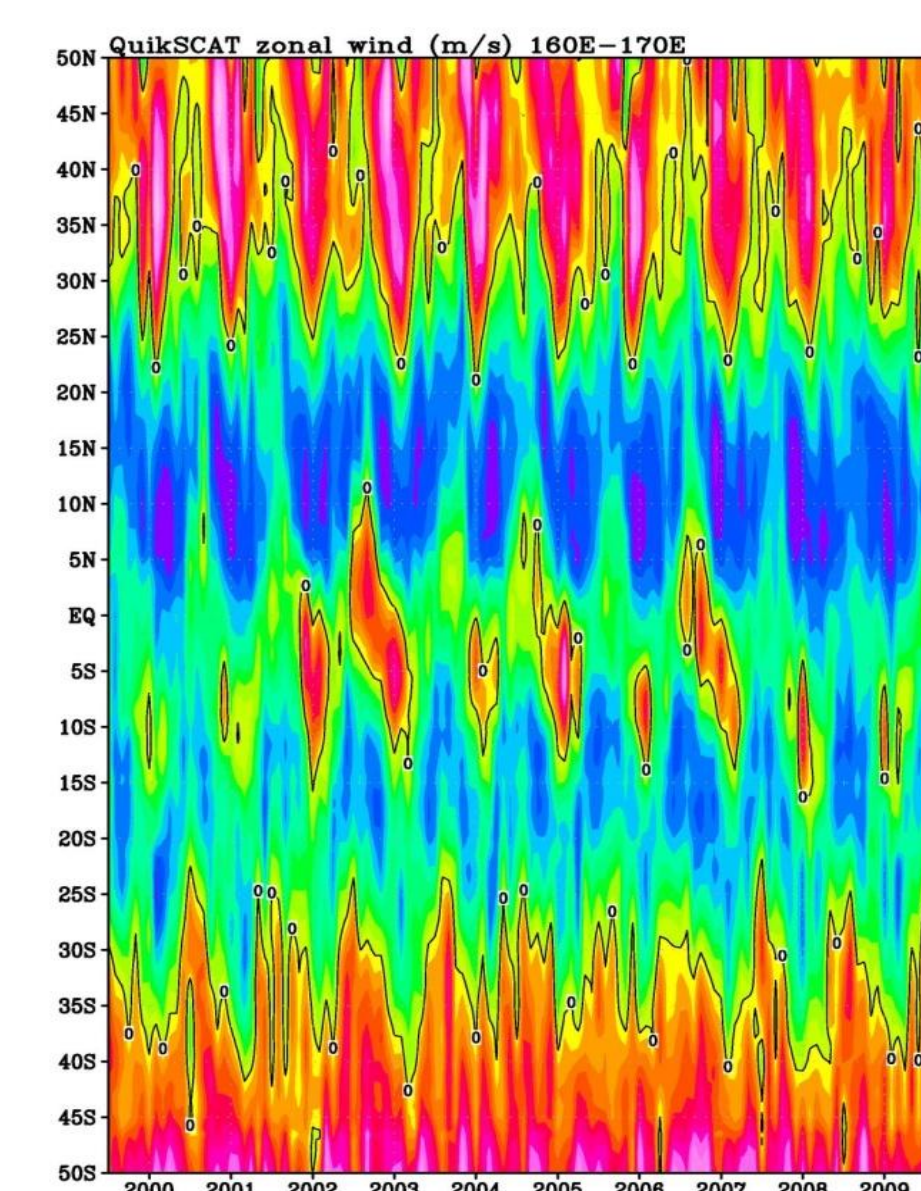
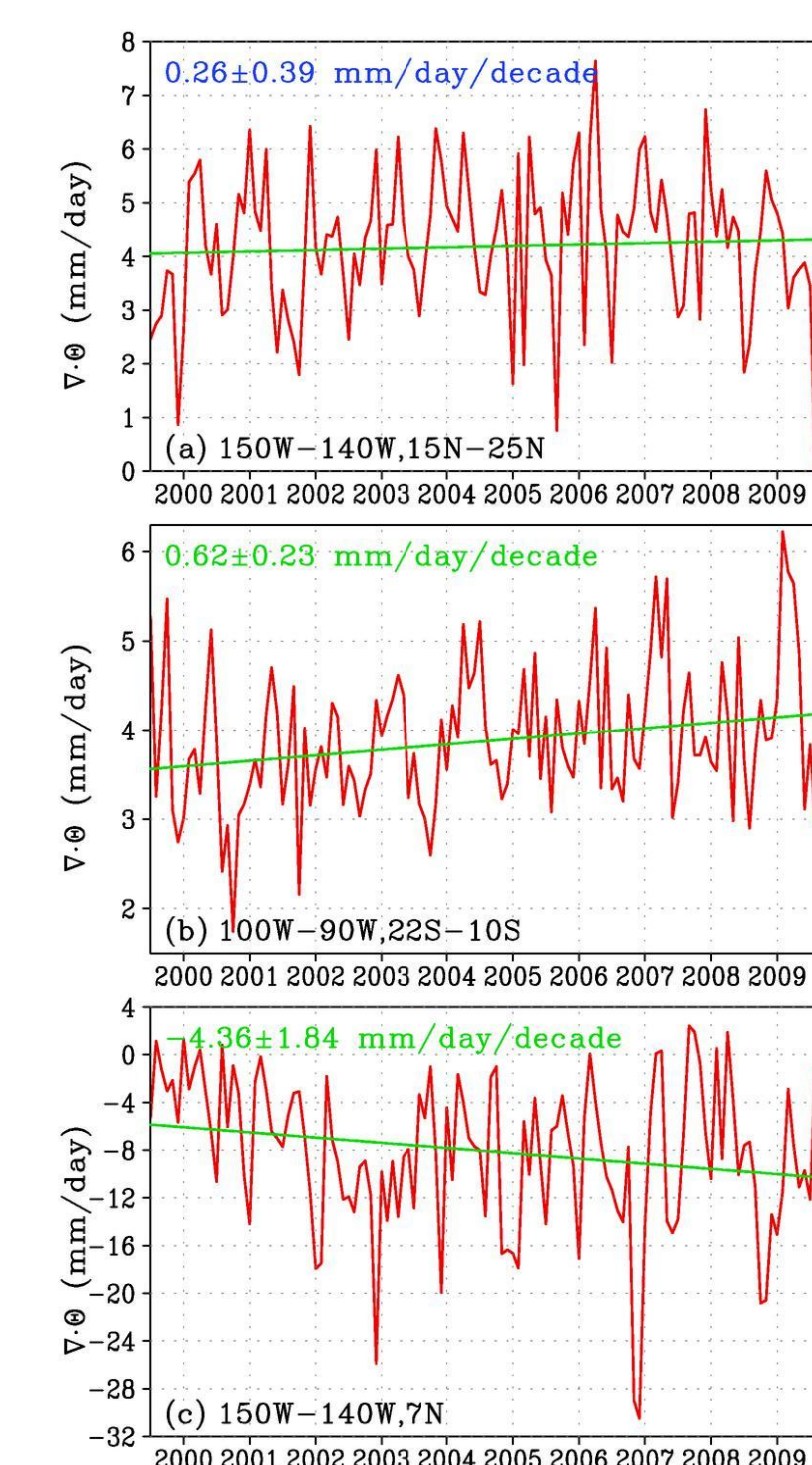


Fig. 6 Hovmoller diagram of zonal component of ENW observed by QuikSCAT averaged between 160°E-170°W.

Regional uncertainties exist. More accurate data are needed.

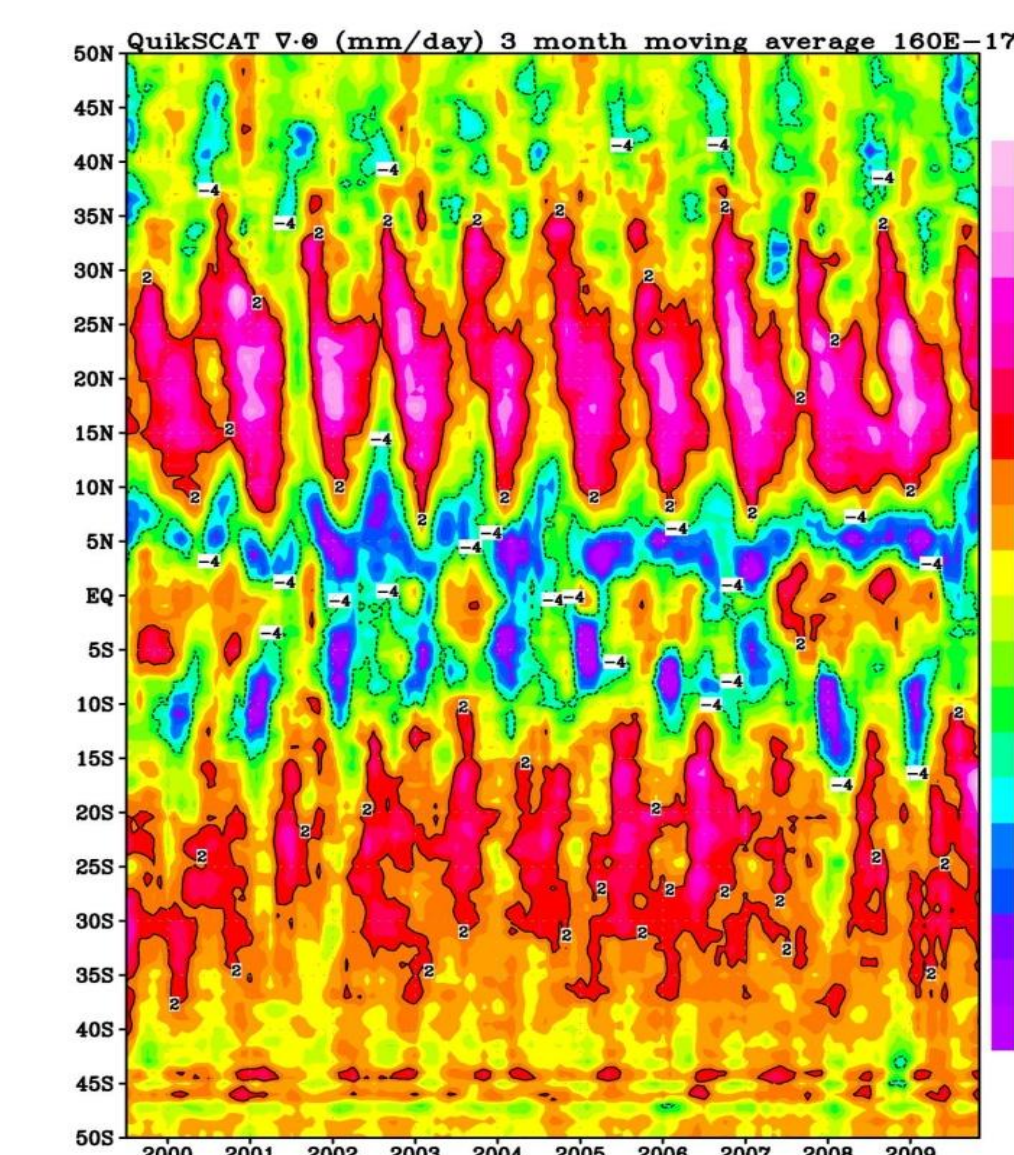


Fig. 7 Same as Fig. 6, except for $-\nabla \cdot \Theta$. A 3-month moving average is applied.

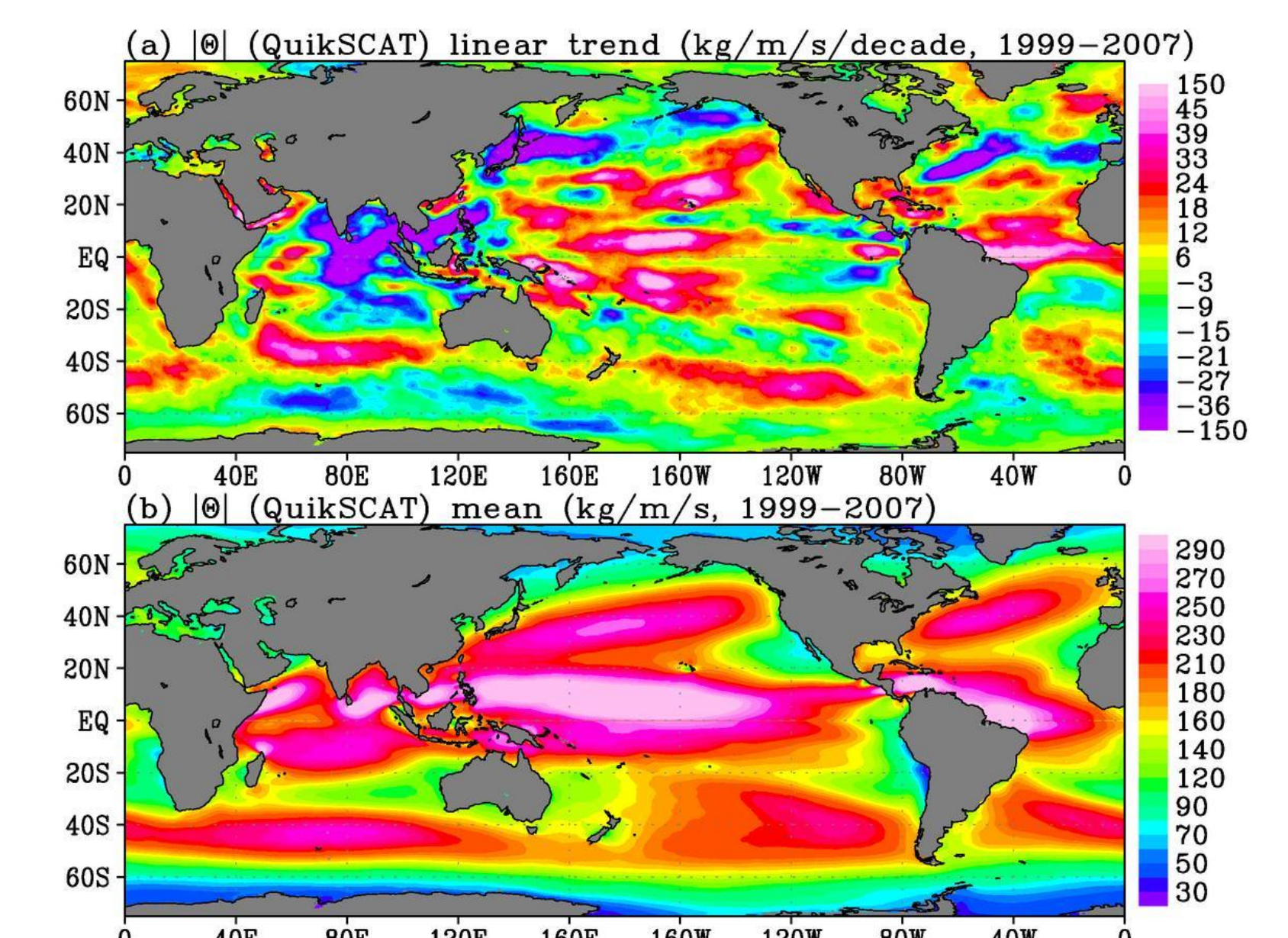


Fig. 8 Linear trend of magnitude of Θ (a), and mean of Θ for period 1999-2009. High magnitude of Θ in North Pacific and North Atlantic are referred to as the atmospheric river that has strong North America and European rainfall. They show positive trend in the past decade.